

Roberge-Weiss transition in $N_f = 2$ QCD with staggered fermions and $N_\tau = 6$

Owe Philipsen

Institut für Theoretische Physik - Johann Wolfgang Goethe-Universität

Max-von-Laue-Str. 1, 60438 Frankfurt am Main

E-mail: philipsen@th.physik.uni-frankfurt.de

Alessandro Sciarra*

Institut für Theoretische Physik - Johann Wolfgang Goethe-Universität

Max-von-Laue-Str. 1, 60438 Frankfurt am Main

E-mail: sciarra@th.physik.uni-frankfurt.de

The QCD phase diagram at imaginary chemical potential exhibits a rich structure and studying it can constrain the phase diagram at real values of the chemical potential. Moreover, at imaginary chemical potential standard numerical techniques based on importance sampling can be applied, since no sign problem is present. In the last decade, a first understanding of the QCD phase diagram at purely imaginary chemical potential has been developed, but most of it is so far based on investigations on coarse lattices ($N_\tau = 4$, $a = 0.3$ fm). Considering the $N_f = 2$ case, at the Roberge-Weiss critical value of the imaginary chemical potential, the chiral/deconfinement transition is first order for light/heavy quark masses and second order for intermediate values of the mass: there are then two tricritical masses, whose position strongly depends on the lattice spacing and on the discretization. On $N_\tau = 4$, we have the chiral $m_\pi^{\text{tric.}} = 400$ MeV with unimproved staggered fermions and $m_\pi^{\text{tric.}} \gtrsim 900$ MeV with unimproved pure Wilson fermions. Employing finite size scaling we investigate the change of this tricritical point between $N_\tau = 4$ and $N_\tau = 6$ as well as between Wilson and staggered discretizations.

The 34th annual International Symposium on Lattice Field Theory

24-30 July 2016

University of Southampton, UK

*Speaker.

1. Introduction

The structure of the phase diagram of QCD at zero chemical potential has been studied for more than a decade by now. Investigations both in the chiral ($m \rightarrow 0$) and quenched ($m \rightarrow \infty$) limits are interesting on their own, since they allow to understand the influence of confinement and chiral symmetry breaking on the thermal transition. The structure of the Columbia plot which emerges from studies on very coarse lattices [1, 2, 3] is qualitatively the same for different formulations and lattice spacings: The order of the phase transition for light and heavy quarks is first order, while it becomes a crossover for intermediate values of the mass. Nevertheless, quite significant discrepancies regarding the position of the Z_2 lines separating these regions have been found using different fermions discretizations and no continuum extrapolation of any feature is available.

Introducing a purely imaginary chemical potential and varying it between $\mu_i = 0$ and the Roberge-Weiss critical value, the first-order regions (crossover region) of the Columbia plot continuously enlarge (shrinks), ending in first-order triple (second-order) regions at $\mu_i = \mu_i^{\text{RW}} = T \cdot \pi/3$, because of the Roberge-Weiss symmetry,

$$Z\left(\frac{\mu_i}{T}\right) = Z'\left(\frac{\mu_i}{T} + \frac{2\pi k}{3}\right).$$

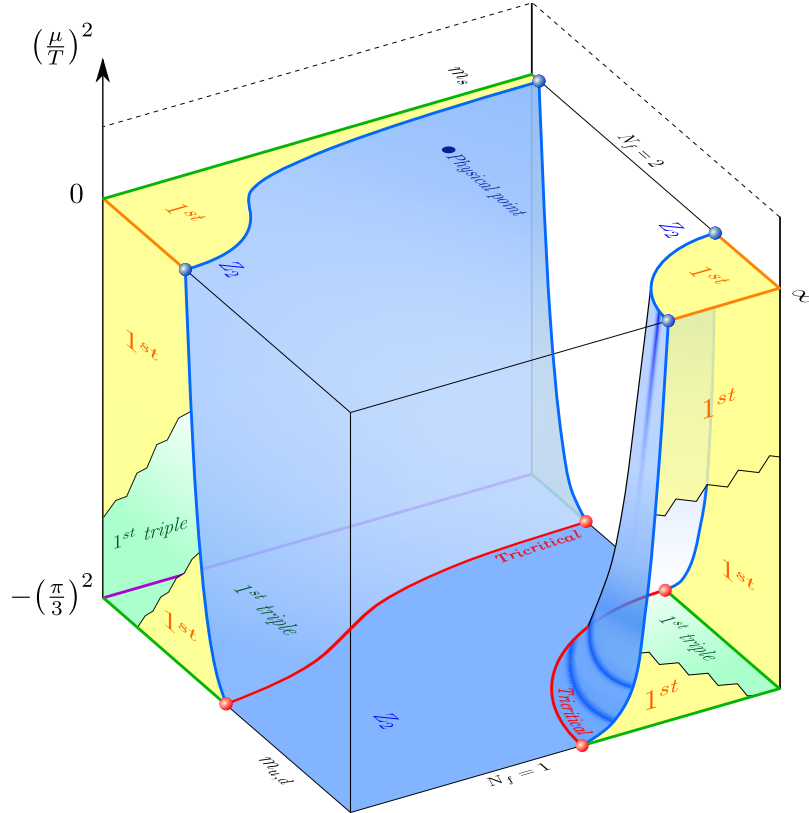


Figure 1: Possible scenario of the 3D Columbia plot. The region below the $\mu = 0$ plane is free from the sign problem and it can be directly studied. The first-order regions on the front vertical planes have been interrupted, in order to allow a better understanding of the picture.

The Z_2 lines change their nature as well, becoming tricritical lines. In Figure 1, a possible scenario of the so-called 3D Columbia plot has been drawn. Even though it corresponds to the findings of previous studies, on finer lattices, the chiral first-order region seems to shrink and it has not been ruled out that it could disappear in the continuum limit, with a consequent second-order phase transition for massless quarks [4].

Focusing on the Roberge-Weiss plane with $N_f = 2$ degenerate quarks, the position of the tricritical points separating the first-order triple regions from the Z_2 one has been found in the last years on $N_\tau = 4$ lattices both with unimproved Wilson fermions [5] and with unimproved staggered fermions [6]. In the first case, this study has been already repeated on $N_\tau = 6$, finer lattices [7] and a comparison between the values of the light tricritical pion masses on the coarser and finer lattices shows that cut-off effects are still large. It is interesting to observe that the chiral $m_\pi^{\text{tric.}} = 400 \text{ MeV}$ with unimproved staggered fermions found on $N_\tau = 4$ lattices is already lighter than that found on $N_\tau = 6$ lattices ($m_\pi^{\text{tric.}} = \text{MeV}$) with unimproved staggered fermions. A better understanding is clearly needed and having the values of $m_\pi^{\text{tric.}}$ on a finer lattice with staggered fermions is a first step in this direction.

2. Simulation details

A standard way to simulate $N_f = 2$ degenerate flavors of staggered fermions is to use the RHMC algorithm [8]. In the present study we used a GPU implementation of it present in the CL²QCD software, a OpenCL based code which is publicly available¹ and that has been optimised to run efficiently on AMD graphic cards [9]. All our simulations were run on the L-CSC cluster [10] in Darmstadt.

Our numeric setup, aside from the different fermion discretization, is completely analogous to that used in [7]. The fourth standardized central moment of the imaginary part of the (spatially averaged) Polyakov loop,

$$B_4(L_{\text{Im}}) \equiv \frac{\langle (\delta L_{\text{Im}})^4 \rangle}{\langle (\delta L_{\text{Im}})^2 \rangle^2} \quad \text{with} \quad \delta L_{\text{Im}} \equiv L_{\text{Im}} - \langle L_{\text{Im}} \rangle ,$$

also known as kurtosis, has been used to identify the nature of the Roberge-Weiss end- or meeting point. Working at $\mu_i^{\text{RW}}/T = \pi$ (i.e. on the second Roberge-Weiss plane), L_{Im} can be used as order parameter and its kurtosis is expected to vary from 3 (crossover) for low temperature to 1 (first order) for high temperature. On finite spatial volumes, B_4 will be a smooth function, becoming discontinuous only in the thermodynamic limit,

$$B_4(\beta) = 2 \Theta(\beta_c - \beta) .$$

Close enough to the critical temperature, if finite size effects are negligible, the kurtosis of L_{Im} is a function of $x \equiv (\beta - \beta_c) N_\sigma^{1/\nu}$ only, where ν is a critical exponent associated to the phase transition. Therefore,

$$B_4(\beta, N_\sigma) = B_4(\beta_c, \infty) + a_1 x + \mathcal{O}(x^2)$$

¹ <https://github.com/CL2QCD/cl2qcd>

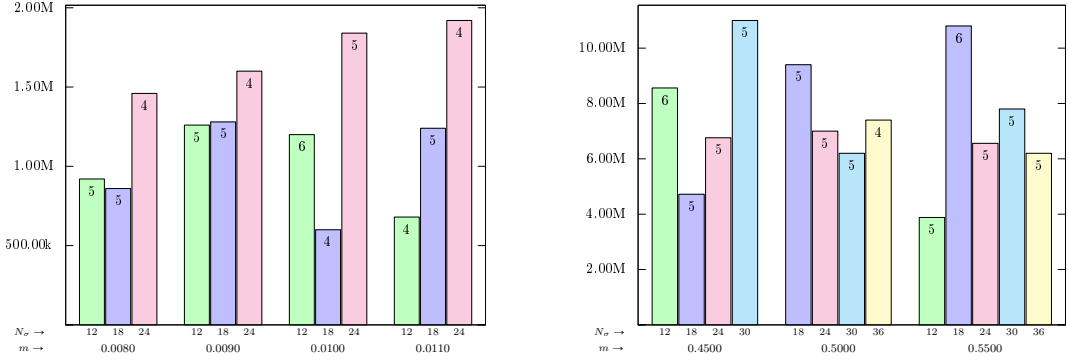


Figure 2: Example of collected statistics per volume at some of the simulated masses. The number written inside each histogram bar indicates the number of simulated β around the critical one for the given volume. Observe the different vertical scales in the light and heavy regions.

and the order of the phase transition can be understood performing a linear fit of our data and looking at ν , which takes its universal value depending on the transition.

In order to locate the two tricritical points, a scan in mass is needed. For each value of $m_{u,d}$, we simulated at a fixed temporal lattice extent $N_\tau = 6$ and at a fixed value of the chemical potential $a\mu_i^{\text{RW}} = \pi/6$. In the finite size scaling analysis, the three larger simulated volumes have been used, always with $N_\sigma \geq 12$ (up to $N_\sigma = 36$). For each lattice size, 3 to 8 values of β around the critical temperature have been simulated, each with 4 Markov chains. The accumulated statistics per β has not been constant since we adopted two different precisions to decide when to stop our simulations in the light and in the heavy regions. In particular, for large (small) masses we required the kurtosis of the imaginary part of Polyakov loop to be the same on all the chains within 2 (3) standard deviations. Since this condition can be met for poor statistics because of large errors, as rough rule of thumb, we required all the 4 values of the kurtosis at a given temperature to span with their error an interval not wider than 0.5. In Figure 2, the total number of unitary trajectories produced per volume at 8 of the 18 simulated mass values is reported.

Since to understand the order of the phase transition at a given value of the mass is not immediate (both in terms of time and numerical resources), previous studies [1, 6] can help in choosing how to perform the scan in $m_{u,d}$. In particular, at $\mu = 0$ with 3 degenerate flavors of staggered fermions, it has been observed that the Z_2 chiral critical bare mass in lattice units on $N_\tau = 6$ lattices is ~ 7.5 times smaller than that found using $N_\tau = 4$. Supposing a similar behavior also for the chiral tricritical mass μ_i^{RW} , then $m_{\text{light}}^{\text{tric}} = 0.043$ found on $N_\tau = 4$ lattices would imply $m_{\text{light}}^{\text{tric}} = 0.0057$ using $N_\tau = 6$.

3. Analysis and preliminary results

The procedure used to extract the critical exponent ν as well as the value of the kurtosis at β_c in the infinite volume limit is the same used in [7] and we refer to it for a detailed explanation. The basic idea is to use the Ferrenberg-Swendsen reweighting [11] to add few points between simulated β and to fit simultaneously $B_4(\beta, N_\sigma)$ on several spatial volumes linearly around β_c . In order to safely trust the outcome of the fit, finite size effects should not be dominant, i.e. the

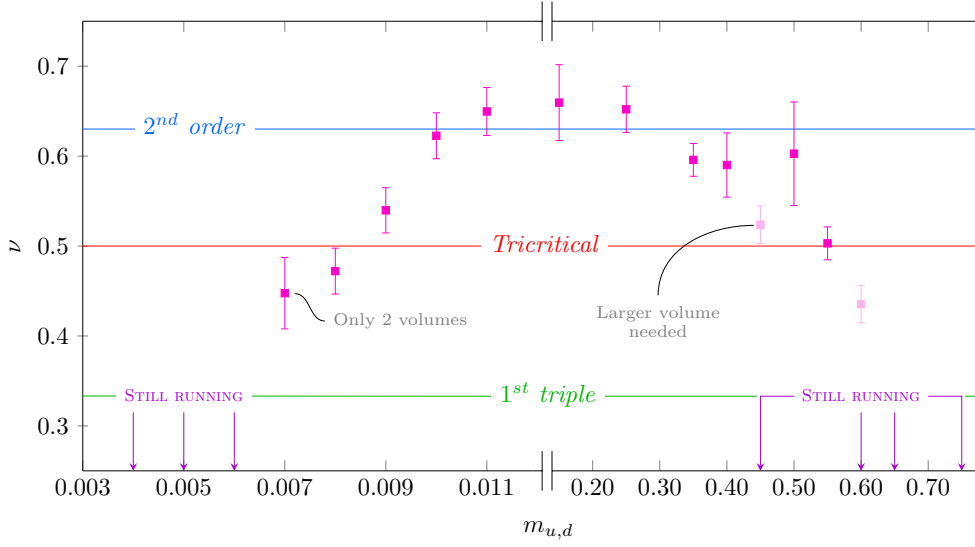


Figure 3: Critical exponent ν as function of the bare quark mass m . The horizontal colored lines are the critical values of ν for some universality classes. The mass axis has been broken and two different scales have been used in order to improve readability. Shaded points have to be considered preliminary.

kurtosis measured on different volumes should meet at the same critical β_c . Whenever this does not happen, a new larger spatial volume is needed and the smallest one should not be included in the finite size scaling analysis. On the other hand, having data on three different N_σ meeting at the same temperature, does not ensure the absence of any finite size correction and a check of the stability of the fit result leaving out the smaller volume is encouraged.

In Figure 3 the extracted values of the critical exponent ν have been plotted for different bare quark masses. As it has been already seen in previous studies [6, 7], leaving the second-order region requires larger spatial volumes to be considered. In particular, the smallest spatial lattice extent for the masses that can be considered finished has been $N_\sigma = 12$ for $m_{u,d} \in [0.008, 0.35]$, $N_\sigma = 18$ for $m_{u,d} \in \{0.007, 0.4\}$ and $N_\sigma = 24$ for $m_{u,d} = \{0.5, 0.55\}$. Despite some simulations are still running and, thus, some points are missing and some others are only preliminary, the expected behavior of ν can be seen. In fact, a second order region for intermediate mass values separates two first-order triple regions. A first conservative estimate of the position of the two tricritical masses can be done,

$$m_{\text{light}}^{\text{tric}} = 0.008_{-0.003}^{+0.002} \quad \text{and} \quad m_{\text{heavy}}^{\text{tric}} = 0.55(10) \quad .$$

The lack of points in the chiral region led us to choose an asymmetric error for the light tricritical mass. In the deconfinement region, instead, $m_{u,d} = 0.45$ has been considered as lower bound for the tricritical point, even though the fit analysis gives a value of ν quite similar to the tricritical one. This choice is due to the fact that more information can be gathered looking at the collapse plot of the kurtosis of the imaginary part of the Polyakov loop – i.e. plotting $B_4(L_{\text{Im}})$ as a function of the scaling variable $x \equiv (\beta - \beta_c) N_\sigma^{1/\nu}$ at fixed β_c and ν . Since the data on the two largest volumes have a better collapse for $\nu = 0.63$ than for $\nu = 0.5$, we are confident that at this mass the system undergoes a second-order phase transition in the thermodynamic limit and adding a larger volume will clarify the situation.

4. Conclusions and perspectives

A preliminary comparison between the position of the tricritical masses on $N_\tau = 4$ and $N_\tau = 6$ lattices can be done in terms of $m_{u,d}/T = N_\tau am_{u,d}$. In the chiral region, the tricritical point moves

N_τ	$m_{\text{light}}^{\text{tric}}/T$	$m_{\text{heavy}}^{\text{tric}}/T$
4	0.172(20)	2.9(3)
6	$0.048^{+0.012}_{-0.018}$	3.3(6)

towards smaller masses as already observed in previous studies with different discretizations, but the shift seems to be milder than at $\mu = 0$ with three degenerate flavors of staggered fermions. $m_{\text{heavy}}^{\text{tric}}/T$, instead, seems not to change and compatible values on $N_\tau = 4$ and $N_\tau = 6$ lattices are found.

Clearly, to draw any conclusion, some more work is needed. In first place the missing points in Figure 3 will help to confirm the position of the tricritical masses. Furthermore, the measurement of the pion mass and of the lattice spacing for each of the simulated quark bare masses is ongoing and this will allow a comparison with results obtained with different fermion discretizations, too.

Finally, the outcome of this study suggests that further investigations on even finer lattices in the chiral region are increasingly prohibitive. The range of bare mass values to be simulated will probably further shift towards smaller values and it is known that this implies more costly simulations. Moreover, increasing N_τ , larger spatial extents will be needed in order to perform the finite scaling analysis. Consequently, new algorithmic improvements are required. On the other hand, in the heavy mass region, it would be interesting to check whether the ratio $m_{\text{heavy}}^{\text{tric}}/T$ stays constant even on finer lattices. Even though this would still imply to simulate smaller bare quark masses and to use larger spatial volumes, it seems to be a feasible task. However, it has to be checked if the lattice spacings used so far are fine enough to resolve the pion, i.e. whether $am_\pi < 1$. Recent studies both at $\mu = 0$ and at $\mu_i = \mu_i^{\text{RW}}$ with Wilson fermions [7, 12] have found that this is not the case and that in the deconfinement region larger values of N_τ are needed. Of course, different fermions discretizations are affected by different cut-off effects and the situation with staggered fermions could be different. However, considering for instance past investigations on the equation of state for physical quark masses, it turned out that lattice temporal extents $N_\tau \sim 12$ were needed to perform a continuum extrapolation (see [13] and references therein). Forthcoming results are going to clarify also this aspect.

Acknowledgments

We thank the staff of L-CSC for computer time and support. This work is supported by the Helmholtz International Center for FAIR within the LOEWE program of the State of Hesse.

References

- [1] P. de Forcrand, S. Kim and O. Philipsen, *A QCD chiral critical point at small chemical potential: Is it there or not?*, *PoS LAT2007* (2007) 178, [[0711.0262](#)].
- [2] C. Bonati, P. de Forcrand, M. D’Elia, O. Philipsen and F. Sanfilippo, *Chiral phase transition in two-flavor QCD from an imaginary chemical potential*, *Phys. Rev.* **D90** (2014) 074030, [[1408.5086](#)].
- [3] WHOT-QCD collaboration, H. Saito, S. Ejiri, S. Aoki, T. Hatsuda, K. Kanaya, Y. Maezawa et al., *Phase structure of finite temperature QCD in the heavy quark region*, *Phys. Rev.* **D84** (2011) 054502, [[1106.0974](#)].
- [4] P. de Forcrand, *Continuum limit and universality of the Columbia plot*, in *Proceedings, 34th International Symposium on Lattice Field Theory (Lattice 2016): Southampton, UK, July 24-30, 2016*.
- [5] O. Philipsen and C. Pinke, *Nature of the Roberge-Weiss transition in $N_f = 2$ QCD with Wilson fermions*, *Phys. Rev.* **D89** (2014) 094504, [[1402.0838](#)].
- [6] C. Bonati, G. Cossu, M. D’Elia and F. Sanfilippo, *The Roberge-Weiss endpoint in $N_f = 2$ QCD*, *Phys. Rev.* **D83** (2011) 054505, [[1011.4515](#)].
- [7] C. Czaban, F. Cuteri, O. Philipsen, C. Pinke and A. Sciarra, *Roberge-Weiss transition in $N_f = 2$ QCD with Wilson fermions and $N_\tau = 6$* , *Phys. Rev.* **D93** (2016) 054507, [[1512.07180](#)].
- [8] A. D. Kennedy, I. Horvath and S. Sint, *A New exact method for dynamical fermion computations with nonlocal actions*, *Nucl. Phys. Proc. Suppl.* **73** (1999) 834–836, [[hep-lat/9809092](#)].
- [9] O. Philipsen, C. Pinke, A. Sciarra and M. Bach, *CL^2 QCD - Lattice QCD based on OpenCL*, *PoS LATTICE2014* (2014) 038, [[1411.5219](#)].
- [10] D. Rohr, M. Bach, G. Neskovic, V. Lindenstruth, C. Pinke and O. Philipsen, *Lattice-csc: Optimizing and building an efficient supercomputer for lattice-qcd and to achieve first place in green500*, in *High Performance Computing - 30th International Conference, ISC High Performance 2015, Frankfurt, Germany, July 12-16, 2015, Proceedings*, pp. 179–196, 2015. [DOI](#).
- [11] A. M. Ferrenberg and R. H. Swendsen, *Optimized Monte Carlo analysis*, *Phys. Rev. Lett.* **63** (1989) 1195–1198.
- [12] C. Czaban and O. Philipsen, *The QCD deconfinement critical point for $N_\tau = 8$ with $N_f = 2$ flavours of unimproved Wilson fermions*, in *Proceedings, 34th International Symposium on Lattice Field Theory (Lattice 2016): Southampton, UK, July 24-30, 2016*, 2016. [1609.05745](#).
- [13] O. Philipsen, *The QCD equation of state from the lattice*, *Prog. Part. Nucl. Phys.* **70** (2013) 55–107, [[1207.5999](#)].